Xiong et al. Nanoscale Research Letters (2017) 12:625
DOI 10.1186/s11671-017-2394-0

Nanoscale Research Letters

NANO EXPRESS Open Access

Probing the Structural, Electronic, and Magnetic Properties of Ag_nV ($n = 1–12$) Clusters

Ran Xiong, Dong Die*, Lu Xiao, Yong-Gen Xu* and Xu-Ying Shen

Abstract

The structural, electronic, and magnetic properties of Ag_nV ($n = 1–12$) clusters have been studied using density functional theory and CALYPSO structure searching method. Geometry optimizations manifest that a vanadium atom in low-energy Ag_nV clusters favors the most highly coordinated location. The substitution of one V atom for an Ag atom in Ag_{n+1} ($n \geq 5$) cluster modifies the lowest energy structure of the host cluster. The infrared spectra, Raman spectra, and photoelectron spectra of Ag_nV ($n = 1–12$) clusters are simulated and can be used to determine the most stable structure in the future. The relative stability, dissociation channel, and chemical activity of the ground states are analyzed through atomic averaged binding energy, dissociation energy, and energy gap. It is found that V atom can improve the stability of the host cluster, Ag_2 excepted. The most possible dissociation channels are $Ag_nV = Ag + Ag_{n-1}V$ for $n = 1$ and 4–12 and $Ag_nV = Ag_2 + Ag_{n-2}V$ for $n = 2$ and 3. The energy gap of Ag_nV cluster with odd n is much smaller than that of Ag_{n+1} cluster. Analyses of magnetic property indicate that the total magnetic moment of Ag_nV cluster mostly comes from V atom and varies from 1 to 5 μ_B. The charge transfer between V and Ag atoms should be responsible for the change of magnetic moment.

Keywords: Ag_nV cluster, Growth behavior, Spectrum, Electronic and magnetic property

Background

In the past decades, silver clusters have drawn special attention because of their unusually optical and catalytic properties [1–20]. Simultaneously, theoretical and experimental investigations have revealed that an atom doped into a small cluster of another element can fundamentally change the nature of the host cluster [21–44]. Silver clusters doped with different atoms have been expected to tailor the desired optical, electronic, and magnetic properties for potential applications in imaging, sensing, biology, medicine, and nanotechnology [45–55]. For instance, Si doping into silver cluster leads to a broadening and damping of the peaks of UV-visible absorption spectra of Ag clusters [45]. The optical character of Ag_nAu_m can be adjusted by changing the ratio of silver atoms to gold atoms and Au_4Ag_4 might be a potentially promising molecular photoelectric device [46]. In contrast with silver clusters, the binary Ag-Au cluster-modified TiO_2 electrode improves short-circuit current density and maximum power conversion efficiencies of solar cell [47]. The adsorption energies of a set of typical ligands (–COOH, –CN, –OH, –SH, $–CH_3$, $–NO_2$, $–NH_3$, –NO) are smaller on $Ag_{12}Au$ cluster than on Ag_{13} cluster [48]. Ag-Cu nanoalloy is a potential candidate to substitute noble Pt-based catalyst in alkaline fuel cells [49]. The electrons in outer atoms of $Ag_{12}Cu$ cluster have a more active characteristic than that of Ag_{13} cluster [50]. The catalytic activity of Ag-Pd alloy cluster for hydrogen dissociation is closely associated with the stoichiometry. The Ag_6Pd_2 is the most efficient cluster for hydrogen molecule adsorption and can serve as a promising candidate for H_2 storage [51]. The introduction of a single 3d transition-metal atom effectively solved the instability problem of the Ag_{12} icosahedron [52]. Recently, several investigations have been carried out for V-doped silver clusters on account of their unique physical and chemical properties [56–59]. Zhang et al. reported that the neutral $Ag_{12}V$ cluster show larger relative binding energies compared with pure icosahedral Ag_{13} cluster [56]. Chen et al. found that Pyridine on $V@Ag_{12}^-$ clusters exhibits the strongest chemical enhancement with a factor

* Correspondence: science_dd@163.com; xuyonggen06@163.com
School of Science, Xihua University, Chengdu 610039, China

of about a thousand [57]. Medel et al. explored the nature of valence transition and spin moment in Ag_nV^+ clusters that have an enhanced stability for $n = 14$ [58]. However, there are relatively few works concerning the neutral V-doped silver clusters. In particular, the various spectra of Ag_nV clusters have not been obtained but would be extremely helpful for the identification of cluster structure. The structural motif of V-doped silver clusters is also needed to be further explored. The change of magnetic moment of magnetic impurity embedded in a nonmagnetic host still is not fully understood. Accordingly, in the present paper, the geometrical, electronic, and magnetic properties of Ag_nV ($n = 1–12$) clusters will be systematically researched through density functional theory (DFT). It is hoped that this work can provide a reference for understanding the relationship between the function and structure of materials and for related experiments.

Methods

The accuracy of distinct exchange-correlation functionals, as implemented in GAUSSIAN09 program package (Frisch, M. J. et al., Wallingford, KY, USA) [60], was first verified by calculations on Ag_2 dimer. The calculated results based on PW91PW91/LanL2DZ (Perdew, J. P. et al., New Orleans, Louisiana, USA) level are in good agreement with experimental findings [61, 62], as summarized in Table 1. On the other hand, test calculations using the different DFT functionals were performed for AgV dimer. Five functionals listed in Table 1 favor the same spin configurations. Thus, this level of theory is used for geometry optimizations and frequency analyses of Ag_nV clusters. A great many initial configurations of Ag_nV clusters were constructed by using CALYPSO which is an efficient structure prediction method [63]. In this method, structural evolution is achieved by particle swarm optimization (PSO) that is a population-based stochastic optimization technique. The bond characterization matrix technique is utilized to enhance searching efficiency and remove similar structures. The significant feature of CALYPSO requires only chemical compositions for a given cluster to predict its structure. Due to the spin polarization effect, each initial structure was optimized at possible spin states. If an imaginary vibrational frequency is found, a relaxation of the unstable structure will be done until the local minimum is really obtained. In all computations, the convergence thresholds were set to 6.0×10^{-5} Å for the displacement, 1.5×10^{-5} Hartree/Bohr for the forces and 10^{-6} Hartree for a total energy.

Results and Discussions

Geometrical Structures and Vibrational Spectra

For Ag_nV ($n = 1–12$) clusters, an extensive structural search has been performed and many isomers have been obtained. The most stable structure and two low-lying isomers for each Ag_nV cluster are displayed in Fig. 1. According to the energies from low to high, these isomers are denoted by na, nb, and nc, where n represents the number of Ag atoms in Ag_nV cluster. Their symmetry, spin multiplicity, and energy difference compared to each of the most stable structures are also indicated in the figure. Some physical parameters of the ground state Ag_nV clusters are gathered in Table 2. Meanwhile, in order to examine the effects of dopant V on silver clusters, geometry optimizations of Ag_n ($n = 2–13$) clusters have been accomplished using the same method and basis set. The lowest energy structures of Ag_n clusters plotted in Fig. 1 agree well with earlier report [39].

The optimized results for AgV dimer show that the quintet spin state is energetically lower than the triplet and septet spin states by 0.92 and 1.47 eV, respectively. Therefore, the quintet AgV is the ground state structure. The most stable structure of Ag_2V cluster is the triangular 2a with C_{2v} symmetry. The 2a configuration in quartet spin state becomes the 2b isomer. The 3a and 4a isomers, which resemble the lowest energy structures of Ag_4 and Ag_5 clusters, are the ground state of Ag_3V and Ag_4V clusters. The ground state structure of Ag_4V cluster is also in accord with the result of Medel et al. [58]. The 4b isomer with V atom on the top is a square pyramid and the first three-dimensional (3D) structure. The 4c isomer possesses a triangular bipyramid structure, and its total energy is above the 4a isomer by

Table 1 The bond length and electronic properties of Ag_2 and V_2 dimers

Dimer	Functional/basis set	R(Å)		D_e(eV)		VIP(eV)		EA(eV)		f(cm^{-1})	
		Calc.	Expt.	Calc.	Expt.	Calc.	Expt.	Calc.	Expt.	Calc.	Expt.
Ag_2	PW91PW91/LanL2DZ	2.58	2.53[a]	1.78	1.65[a]	7.96	7.65[a]	0.97	1.02[a]	187.0	192.4[a]
	PBEPBE/LanL2DZ	2.59		1.76		7.89		0.92		184.2	
	BP86/LanL2DZ	2.58		1.75		8.05		1.08		188.4	
	LSDA/LanL2DZ	2.50		2.35		8.87		1.52		215.2	
	B3LYP/LanL2DZ	2.61		1.55		7.80		0.93		177.0	
V_2	PW91PW91/LanL2DZ	1.78	1.77[b]	2.75	2.47 ± 0.22[b]	6.46	6.35[b]	0.46		657.3	

[a]Ref. [67]
[b]Ref. [68]

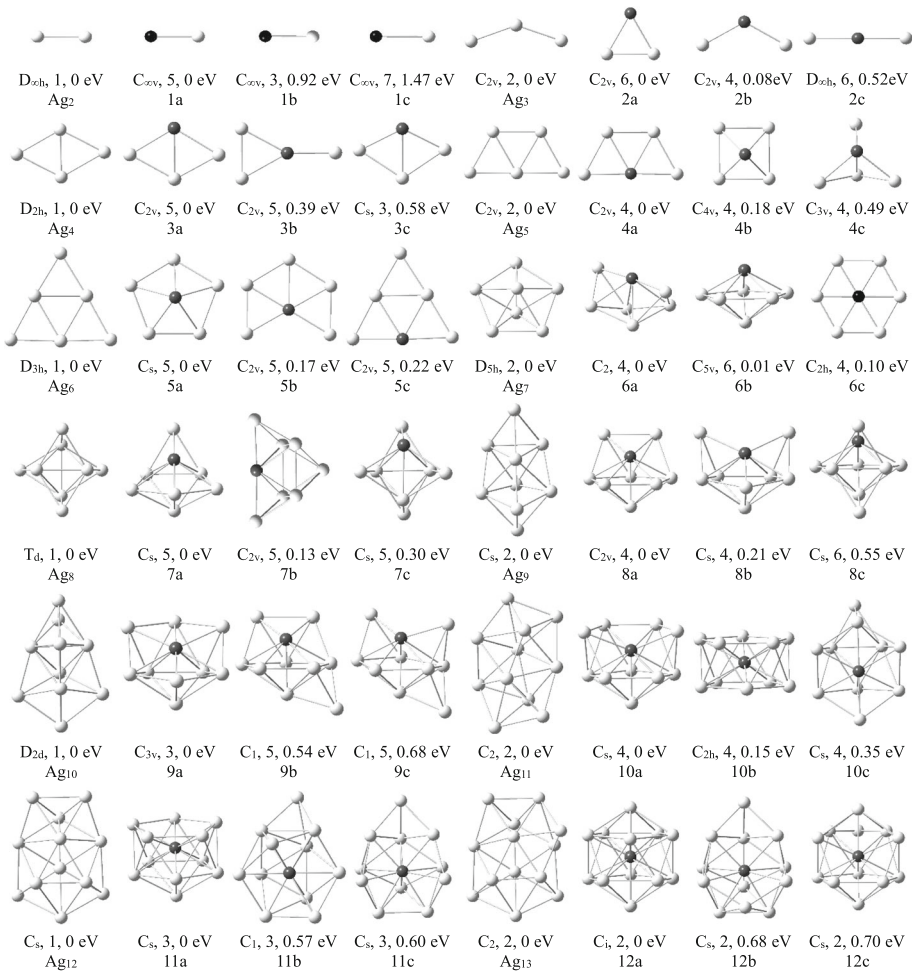

Fig. 1 The ground state structures of Ag_{n+1} and Ag_nV (n = 2–12) clusters. Two low-lying isomers for Ag_nV clusters. The symmetry, spin multiplicity, and energy difference are given below them. The gray and black balls denote Ag and V atoms, respectively

Table 2 The dipole moment (μ), polarizability $\left(a_{xx},\ a_{yy},\ a_{zz},\ \overline{a}\right)$, zero-point energy (ZPE) and maximum and minimum bond lengths (R_{max}, R_{min}) of the most stable Ag_nV (n = 1–12) clusters and coordination number and average coordination bond length (R_v) for V atom

Clusters	μ (D)	a_{xx} (a.u.)	a_{yy} (a.u.)	a_{zz} (a.u.)	$\overline{a}$(a.u.)	ZPE(eV)	N	R_{max} (Å)	R_{min} (Å)	R_v(Å)
AgV	2.07	100.40	100.40	155.87	118.89	0.01	1	2.61	2.61	2.61
Ag_2V	0.89	124.35	182.31	196.44	167.70	0.03	2	2.73	2.72	2.73
Ag_3V	1.42	135.44	277.87	178.70	197.34	0.04	3	2.77	2.71	2.76
Ag_4V	0.82	132.08	340.88	230.06	234.34	0.06	4	2.79	2.70	2.73
Ag_5V	0.62	327.29	292.90	165.77	261.99	0.08	5	2.82	2.70	2.74
Ag_6V	0.74	332.60	325.89	245.02	301.17	0.10	6	2.91	2.72	2.77
Ag_7V	0.21	391.20	340.25	258.36	329.94	0.12	7	3.02	2.73	2.80
Ag_8V	0.35	417.09	378.36	276.02	357.16	0.14	8	2.88	2.77	2.79
Ag_9V	0.41	423.10	423.10	300.90	382.37	0.16	9	2.94	2.75	2.80
$Ag_{10}V$	0.77	424.83	364.25	451.18	413.42	0.18	10	3.01	2.76	2.79
$Ag_{11}V$	0.59	402.07	440.99	442.18	428.41	0.20	11	3.13	2.75	2.77
$Ag_{12}V$	0	440.39	439.34	441.45	440.39	0.22	12	3.04	2.76	2.77

0.49 eV. Other planar and 3D isomers are less stable than 4c isomer.

Starting from $n = 5$, the lowest energy structures of Ag_nV clusters prefer 3D configurations. To prevent from leaving out the ground state, we had also utilized the optimized strategies of substituting an Ag by one V atom from the stable silver cluster or adding Ag atom(s) to small Ag_nV clusters. The 5a and 6a isomers are the most stable structures of Ag_5V and Ag_6V clusters. The two isomers are obtained by distorting the geometry from C_{5v} and C_{2v} to C_s and C_2 point groups, respectively. The 6a isomer is 0.62 eV lower in quartet spin state than in sextet spin state. The 5c and 6b isomers are similar to the ground state structures of pure Ag_6 and Ag_7 clusters. The 6b isomer is almost degenerate with the 6a isomer. Owing to the Jahn–Teller effect, the planar 6c isomer with C_{2h} symmetry has a slight deviation from D_{2h} symmetry.

With regard to Ag_nV ($n = 7–12$) clusters, the number of isomers increases rapidly with the increase of cluster size. The optimized structures indicate that the energies of Ag_nV clusters with the same configuration increase with the decrease of the coordination number of V atom. As a result, various Ag_nV isomers where V atom occupies the position with the highest coordination number were considered further to make sure that the most stable structures are the global minimum. The lowest energy structures of Ag_7V, Ag_8V, Ag_9V, $Ag_{10}V$, $Ag_{11}V$, and $Ag_{12}V$ clusters are 7a, 8a, 9a, 10a, 11a, and 12a in Fig. 1, respectively. Their geometries are qualitatively in accord with results of Medel et al. [58]. These structures are entirely different from the ground state structure of the corresponding Ag_{n+1} clusters and contain a pentagonal bipyramid. The Ag_nV isomers which correspond to the lowest energy structures of Ag_{n+1} clusters lay above each of the ground state structures (na). In addition, the 10b and 12a have a slight deviation from D_{5d} and D_{3d} symmetry. The cage configuration of $Ag_{12}V$ cluster, where V atom occupies the central position, is discovered only in the lowest spin states.

From the optimized results, it is found that the Ag_nV clusters have an obvious growth law. The trapezoid and icosahedron are two basic frameworks for the growth process of Ag_nV cluster, as shown in Fig. 2. The two- to three-dimensional structural transition for Ag_nV cluster occurs at $n = 5$. The transition size of Ag_nV cluster is smaller than that of pure Ag clusters ($n = 6$). For $n = 5–12$, the ground states of Ag_nV clusters are obviously distinct from those of the Ag_{n+1} clusters. The V atom in Ag_nV cluster tends to occupy the most highly coordinated position and is gradually encapsulated in the center by the Ag atoms. This may be attributed to the principle of maximum overlap in chemical bond theory of complexes. Because Ag and V atoms have more orbital overlap under the above circumstances, the energy of Ag_nV cluster, which is also related to the arrangement of Ag atoms, will be lower and then the corresponding cluster is more stable.

The infrared and Raman spectroscopy are powerful tools for the identification of cluster structure and material component. Generally, the structural identification is accomplished by comparing experimental findings with theoretical predictions which is an indispensable part. Accordingly, the infrared spectra and Raman spectra of the most stable Ag_nV ($n = 1–12$) clusters are displayed in Fig. 3. The infrared spectrum shows asymmetric vibrations of polar group. Raman spectrum reveals the symmetric vibrations of nonpolar group and skeleton. The AgV dimer have the same infrared and Raman spectra. For other Ag_nV clusters, the strong absorption location of infrared spectrum has a weak peak in Raman scattering spectrum. On the contrary, the Raman scattering peak is strong and the infrared absorption is weak. The peak position in the two kinds of spectra for all isomers are in the range of 15~270 cm^{-1}. The most intense peak in the infrared

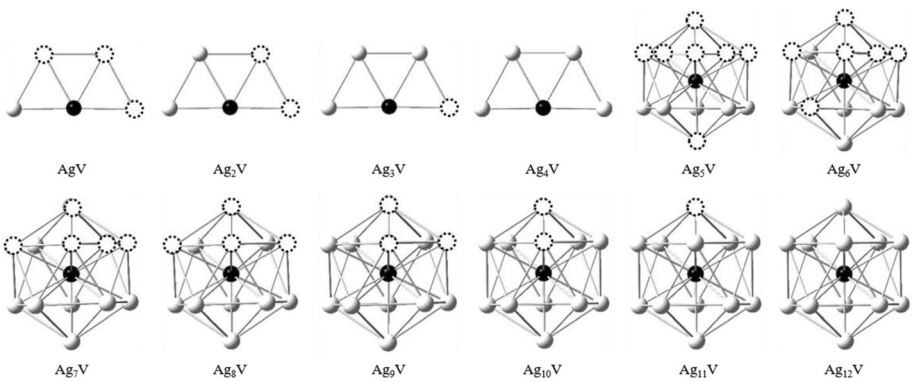

Fig. 2 The growth diagram of Ag_nV ($n = 1–12$) clusters

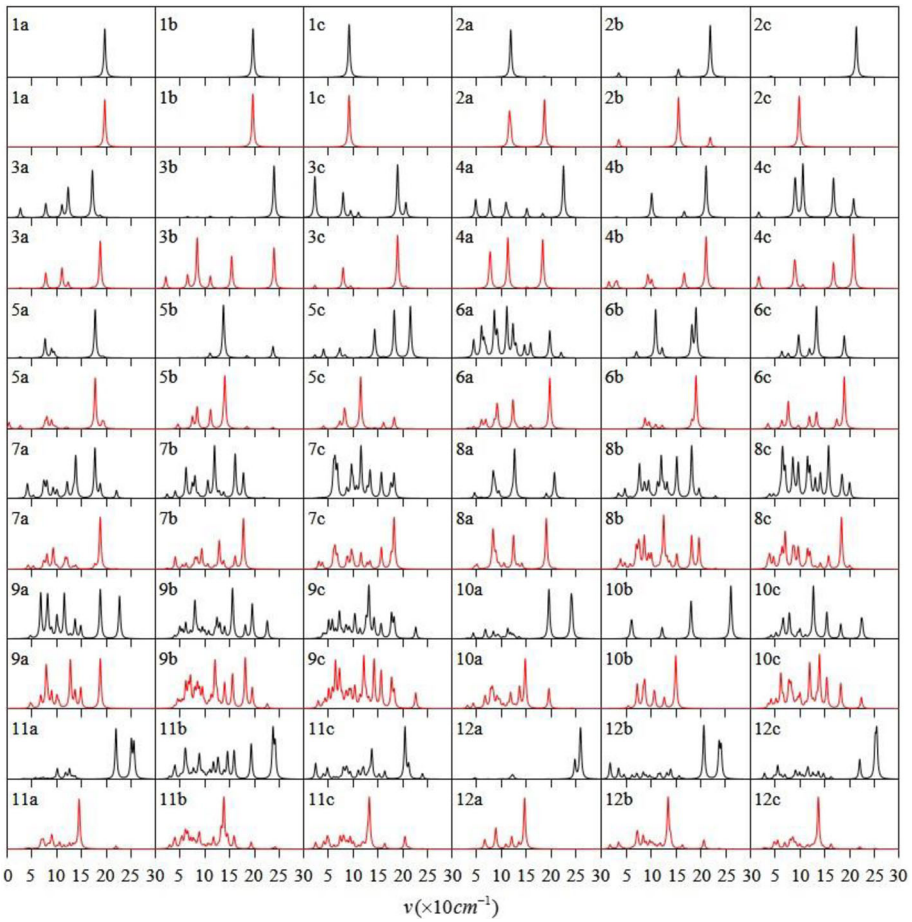

Fig. 3 The infrared spectra (black) and Raman spectra (red) of the ground state and two low-lying isomers of Ag_nV ($n = 1–12$) clusters

spectrum of each Ag_nV clusters is related to the Ag-V stretching vibration.

Electronic Properties

The vertical ionization potential (VIP) and electron affinity (EA) are two primary quantities to probe the electronic properties and can be calculated as follows:

$$\mathrm{VIP} = E(\text{cationic cluster}) - E(\text{cluster}) \quad (1)$$

$$\mathrm{EA} = E(\text{cluster}) - E(\text{anionic cluster}) \quad (2)$$

where E(cationic cluster) and E(anionic cluster) are the single-point energies of cationic and anionic clusters in the geometry of neutral cluster. For the lowest energy Ag_{n+1} and Ag_nV clusters, Table 3 lists the calculated VIP, EA, and the available experimental values. The calculated VIPs and EAs of Ag_{n+1} clusters are in line with their measured data. This consistency confirms the reliability of the current theoretical approach again. Moreover, we note that AgV dimer has the biggest VIP and the smallest EA. This implies that AgV is hard to lose or require an electron. The icosahedral $Ag_{12}V$

Table 3 VIP and VEA of the ground state Ag_{n+1} and Ag_nV clusters. The data in parentheses are experimental findings

Clusters	VIP(eV)	VEA(eV)	Clusters	VIP(eV)	VEA(eV)
Ag_2	7.96	0.97	AgV	7.04	0.82
Ag_3	6.92(6.20[a])	2.17	Ag_2V	5.99	1.28
Ag_4	6.60(6.65[a])	1.63	Ag_3V	6.35	1.49
Ag_5	6.28(6.35[a])	2.04	Ag_4V	6.33	1.86
Ag_6	7.15(7.15[a])	1.33	Ag_5V	6.09	1.47
Ag_7	6.06(6.40[a])	1.94	Ag_6V	6.32	1.87
Ag_8	6.99	1.17	Ag_7V	5.89	1.69
Ag_9	6.01	2.27	Ag_8V	5.79	1.87
Ag_{10}	5.95	1.66	Ag_9V	5.87	2.08
Ag_{11}	5.86	2.42	$Ag_{10}V$	5.88	2.24
Ag_{12}	6.13	2.09	$Ag_{11}V$	5.83	2.31
Ag_{13}	5.61	2.36	$Ag_{12}V$	5.99	2.45

[a]Ref. [67]

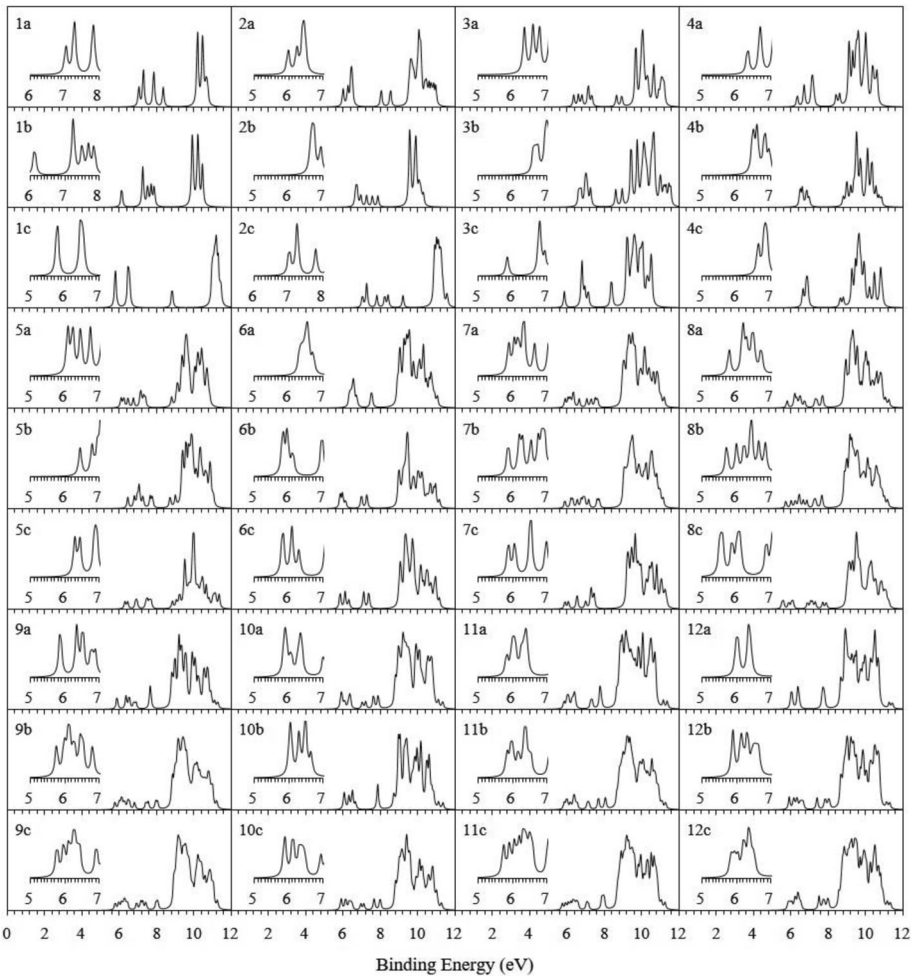

Fig. 4 Simulated PES of the ground state and two low-lying isomers of Ag_nV ($n = 1–12$) clusters

cluster has the biggest EA and is easy to get one more electron. To offer reference material for photoelectron spectroscopy experiment in the aftertime, the theoretical photoelectron spectra (PES) of the ground state and two low-lying structures of Ag_nV ($n = 1–12$) clusters were simulated by adding the first VIP to each occupied orbital energy relative to the HOMO and fitting them with a Lorentz expansion scheme and a broadening factor of 0.1 eV, as shown in Fig. 4. The distribution of energy level of these clusters is in the range of 5.5 to 12 eV. The experimenters can make use of the PES spectra to distinguish these clusters.

In order to examine the influence of V atom on the stability of silver clusters, the atomic averaged binding energies (E_b) of the most stable Ag_{n+1} and Ag_nV clusters can be estimated as follows:

$$E_b(\mathrm{Ag}_{n+1}) = \left[(n+1)E(\mathrm{Ag}) - E(\mathrm{Ag}_{n+1})\right]/(n+1), \quad (3)$$

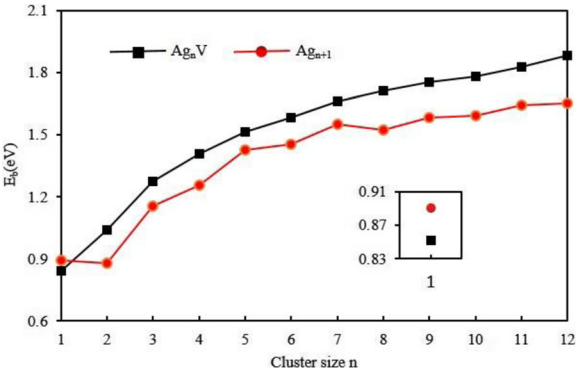

Fig. 5 The averaged binding energies of the lowest energy Ag_{n+1} and Ag_nV ($n = 1–12$) clusters

Table 4 The dissociation energy (D_E, eV) of Ag_nV clusters for the distinct dissociation channels

Ag_nV clusters dissociation channel	D_E $n=1$	D_E $n=2$	D_E $n=3$	D_E $n=4$	D_E $n=5$	D_E $n=6$	D_E $n=7$	D_E $n=8$	D_E $n=9$	D_E $n=10$	D_E $n=11$	D_E $n=12$
$AgV = Ag_n + Ag_{1-n}V$	1.70											
$Ag_2V = Ag_n + Ag_{2-n}V$	1.43	1.36										
$Ag_3V = Ag_n + Ag_{3-n}V$	1.98	1.63	2.48									
$Ag_4V = Ag_n + Ag_{4-n}V$	1.94	2.13	2.72	2.44								
$Ag_5V = Ag_n + Ag_{5-n}V$	2.05	2.21	3.33	2.79	2.82							
$Ag_6V = Ag_n + Ag_{6-n}V$	1.99	2.26	3.35	3.35	3.10	2.53						
$Ag_7V = Ag_n + Ag_{7-n}V$	2.22	2.43	3.63	3.59	3.89	3.05	3.14					
$Ag_8V = Ag_n + Ag_{8-n}V$	2.10	2.54	3.68	3.75	4.02	3.72	3.54	3.14				
$Ag_9V = Ag_n + Ag_{9-n}V$	2.15	2.47	3.84	3.86	4.23	3.90	4.26	3.45	3.84			
$Ag_{10}V = Ag_n + Ag_{10-n}V$	2.03	2.40	3.65	3.90	4.21	3.99	4.31	4.05	4.17	3.75		
$Ag_{11}V = Ag_n + Ag_{11-n}V$	2.35	2.60	3.90	4.02	4.57	4.29	4.72	4.42	5.09	4.39	4.41	
$Ag_{12}V = Ag_n + Ag_{12-n}V$	2.54	3.11	4.29	4.46	4.89	4.84	5.21	5.02	5.65	5.50	5.24	4.80

$$E_b(Ag_nV) = [nE(Ag) + E(V) - E(Ag_nV)]/(n+1), \quad (4)$$

where $E(Ag)$, $E(Ag^{n+1})$, $E(V)$, and $E(Ag_nV)$ are the energies of Ag atom, silver cluster, V atom, and Ag_nV cluster, respectively. The calculated binding energies per atom for the most stable Ag_{n+1} and Ag_nV clusters are plotted in Fig. 5. It is clear from this figure that the E_b of Ag_nV cluster is a monotonically increasing function of the cluster size and larger than that of Ag_{n+1} cluster for $n \geq 2$. Especially, the E_b of doped cluster increase rapidly for the planar structures and gradually for the 3D structures. This means that the bonding force among atoms becomes stronger and stronger in the process of growth. The substitution of a V atom for an Ag atom in $Ag_{n+1}(n \geq 2)$ clusters can evidently enhance the stability of the host clusters. On the other hand, the bond energy of diatomic cluster should be closely related to the bond length. The E_b of AgV dimer is smaller than that of Ag_2. The abnormal change may be ascribed to the fact that the bond distance of AgV (2.61 Å) is longer than that of Ag_2 (2.58 Å).

The thermal stability of clusters can be examined by the dissociation energy (DE), which is different for the distinct dissociation channels. The most basic dissociation channel is the splitting of a larger cluster into two smaller clusters. The corresponding DE is small relative to other dissociation channel. Hence, the subsequent dissociation channels are investigated for the most stable Ag_nV ($n = 1$–12) clusters.

$$Ag_nV \rightarrow Ag_m + Ag_{n-m}V \quad (5)$$

where m is not more than n. The DEs of the above dissociation channels are defined as follows:

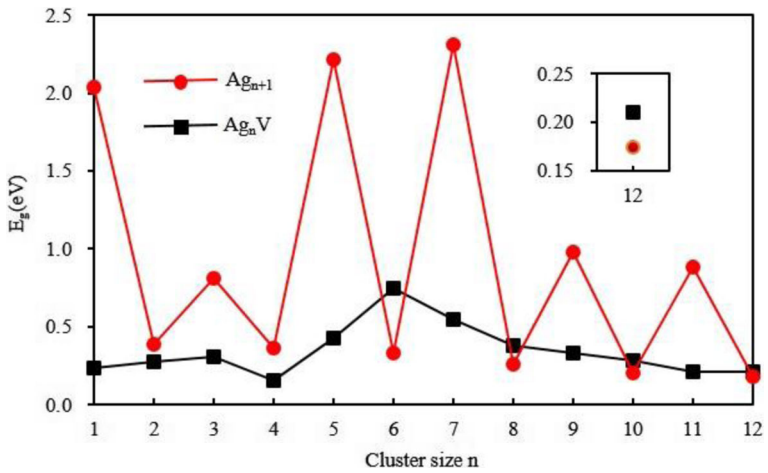

Fig. 6 The HOMO-LUMO energy gaps of the ground state Ag_{n+1} and Ag_nV (n=1–12) clusters

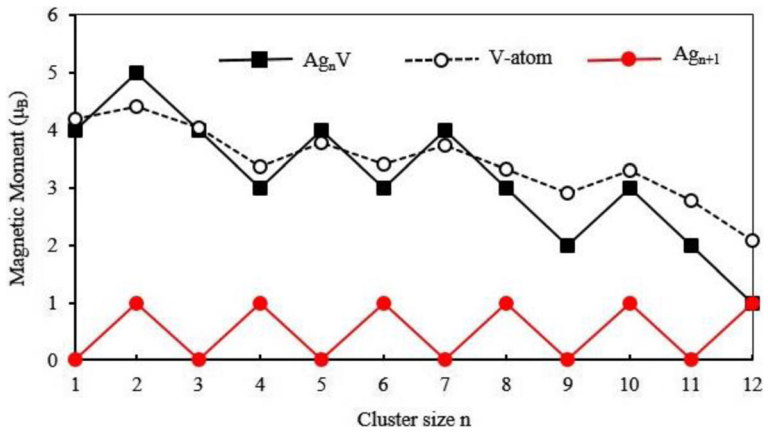

Fig. 7 Total magnetic moment of the ground state Ag_{n+1} and Ag_nV (n = 1–12) clusters and local magnetic moment on V atom

$$DE_m(Ag_nV) = E(Ag_m) + E(Ag_{n-m}V) - E(Ag_nV) \quad (6)$$

where E represents the energy of the corresponding cluster or atom. The DEs of Ag_nV clusters for the different dissociation channels have been listed in Table 4. The small DE indicates that corresponding dissociation channel is easy to take place. That is to say, the dissociation channel corresponding to the minimum DE is most likely to occur. It can be seen from Table 4 that the most preferred dissociation channels of Ag_nV clusters are $Ag_nV = Ag + Ag_{n-1}V$ for $n = 1$ and 4–12 and $Ag_nV = Ag_2 + Ag_{n-2}V$ for $n = 2$ and 3. The minimum DE (2.54 eV) of $Ag_{12}V$ cluster is biggest in all doped cluster, implying that the icosahedral cluster is more stable than other cluster. In addition, we find that the change trend of the minimum DE of the 3D neutral Ag_nV (n = 5–12) cluster is the same as that of abundances of the cationic Ag_nV^+ cluster [64, 65]. However, there is no such relationship between planar Ag_nV and Ag_nV^+ for n = 2–4.

The energy gap (E_g) between the highest occupied molecular orbital (HOMO) and lowest unoccupied molecular orbital (LUMO) is always considered to be an important quantity that characterizes the chemical activity of the small metal clusters. A large energy gap is related to a high chemical stability. For the ground state Ag_{n+1} and Ag_nV clusters, Fig. 6 shows the energy gaps as a function of the cluster size. An odd-even alternation is observed in the energy gaps of pure silver clusters. This alternation can be explained by the electron pairing effect, i.e., the electron shielding effect of two electrons occupying the same HOMO is much smaller than that of two electrons occupying different orbits. An Ag atom ($[Kr]4f^{14}4d^{10}5s^1$) in

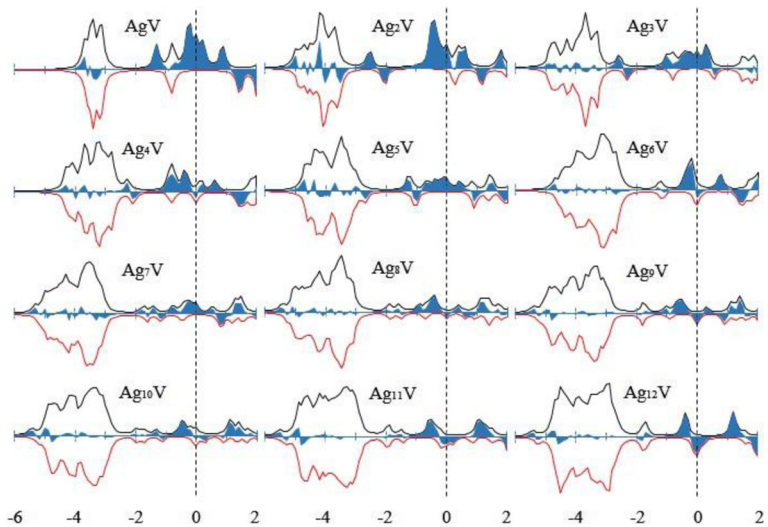

Fig. 8 The SDOS of ground state Ag_nV (n = 1–12) clusters. Spin up is positive and spin down is negative. A broadening factor δ = 0.1 eV is used. Spin up minus spin down is the blue part. The dashed line indicates the location of the HOMO level

Ag_{n+1} cluster is substituted by a V ($[Ar]3d^34s^2$) atom. For odd n, the closed shell of Ag_{n+1} cluster is replaced by the open shell of Ag_nV cluster. Of course, the E_g of Ag_nV cluster with odd n is less than that of Ag_{n+1} cluster. This decrease is very obvious. For even n, both Ag_{n+1} and Ag_nV clusters have an unrestricted shell. The E_g should depend on their structures. In this case, we note that the E_g of Ag_nV ($n = 2$ and 4) cluster with planar structure is smaller than that of Ag_{n+1} cluster and the E_g of Ag_nV ($n = 6$, 8, 10, and 12) cluster with 3D structure is a little bigger than that of Ag_{n+1} cluster. In general, the substitution of one V atom for an Ag atom in Ag_{n+1} clusters with even n has little effect on the energy gap of the host cluster.

Magnetic Properties

The magnetic property of cluster is frequently used in the preparation of nanoelectronic devices and high-density magnetic storage materials. The total magnetic moment of cluster consists of the spin magnetic moment and orbital magnetic moment of electrons. The spin magnetic moment of an electron is much greater than the orbital magnetic moment, and thereby, the magnetic moment of cluster is dominated by the spin magnetic moment. The total magnetic moment of the lowest energy Ag_nV clusters ($n = 1$–12) clusters has been calculated and are presented in Fig. 7, where we have also plotted the total magnetic moment of the host clusters. The magnetic moments of the most stable Ag_{n+1} clusters are completely quenched for odd n and are 1 μ_B for even n. The small Ag_nV clusters have a large magnetic moment. With the increase of the cluster size, the magnetic moment of Ag_nV clusters decreases in waves. When $n = 12$, the $Ag_{12}V$ has the same magnetic moment as Ag_{13} cluster. This means that the doping of V atom can only enhance the magnetism of small silver clusters. As an effort to account for the magnetism, Fig. 8 shows the spin density of states (SDOS) for the ground state Ag_nV clusters. It is obvious from this figure that the Ag_nV clusters have some magnetic domains which decrease with the increase of clusters size. All the lowest energy structures have a strong band between − 5 eV and − 2.5 eV, which is composed mainly of the valence s and d orbitals of the Ag and V atoms. The energy levels near the HOMO, $E - E_{HOMO} = -1$~0 eV, act as a key role in the determination of magnetic behavior of Ag_nV clusters.

To explore the magnetic properties further, we have carried out the natural bond orbital analysis for the most stable Ag_nV clusters [66]. The local magnetic moments on V atom are 4.18 μ_B for AgV, 4.41 μ_B for Ag_2V, 4.03 μ_B for Ag_3V, 3.36 μ_B for Ag_4V, 3.78μ_B for Ag_5V, 3.40 μ_B for Ag_6V, 3.73 μ_B for Ag_7V, 3.33 μ_B for Ag_8V, 2.91 μ_B for Ag_9V, 3.29 μ_B for $Ag_{10}V$, 2.77 μ_B for $Ag_{11}V$, and 2.08 μ_B for $Ag_{12}V$, as shown in Fig. 7. Overall, the magnetic moment of V atom gradually decreases with the size of clusters increasing. The magnetic moment provided by

Table 5 The charge (Q) and local magnetic moment (M) of 4*s*, 3*d*, 4*p*, and 5*d* states for the V atom in the ground state Ag_nV clusters

Clusters	4 *s*–V		3*d*–V		4*p*–V		4*d*–V	
	Q(e)	M (μ_B)	Q(e)	M (μ_B)	Q(e)	M (μ_B)	Q(e)	M (μ_B)
AgV	0.98	0.48	3.79	3.69	0.03	0.01	0	0
Ag_2V	0.81	0.53	3.92	3.82	0.12	0.06	0	0
Ag_3V	0.64	0.32	3.90	3.68	0.25	0.03	0	0
Ag_4V	0.58	0.04	3.77	3.31	0.53	0.01	0.02	0
Ag_5V	0.49	0.07	4.03	3.65	0.82	0.06	0.01	0.01
Ag_6V	0.46	0.04	4.00	3.34	0.92	0.02	0.02	0
Ag_7V	0.47	0.07	4.14	3.56	1.12	0.10	0.02	0
Ag_8V	0.48	0.04	4.22	3.20	1.33	0.09	0.02	0
Ag_9V	0.47	0.03	4.34	2.80	1.53	0.07	0.03	0.01
$Ag_{10}V$	0.50	0.06	4.53	3.11	1.94	0.12	0.04	0
$Ag_{11}V$	0.50	0.04	4.74	2.64	2.25	0.09	0.04	0
$Ag_{12}V$	0.50	0.02	4.97	2.01	2.41	0.05	0.04	0

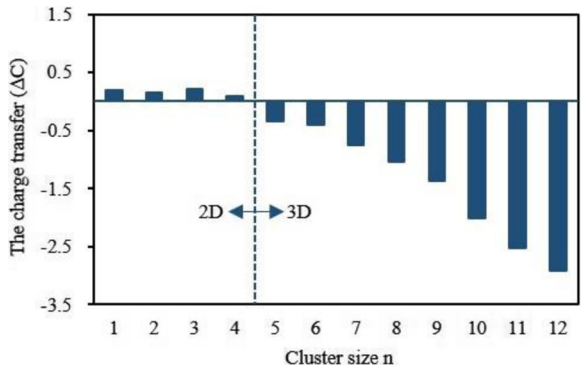

Fig. 9 The charge transfer of V atom in the most stable Ag_nV (n = 1–12) clusters. Free V atom as the reference point

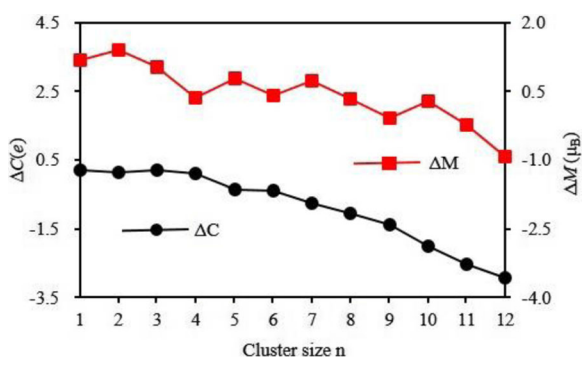

Fig. 10 The charge transfer (ΔC) and the change of magnetic moment (ΔM) of V atom in the most stable Ag_nV (n = 1–12) clusters

Ag atoms is very small. Furthermore, except for Ag_2V, Ag_5V, and Ag_7V clusters, the total magnetic moment of Ag atoms in other doped clusters exhibit the antiferromagnetic alignment with respect to the V atom's magnetic moment. In other words, the total magnetic moments of all Ag_nV clusters are chiefly derived from the paramagnetic V atom, as shown in Fig. 7.

The local magnetic moment and charge on 4*s*, 3*d*, 4*p*, and 4*d* shells of V atom in the lowest energy Ag_nV cluster are listed in Table 5. One can be seen from this table that the partially occupied 3*d* shell play a crucial role in determining the magnetism of V atom and its magnetic moment is 2.01~3.82 μ_B. The 4*s* and 4*p* shells, which are nonmagnetic for a free V atom, produce a little of the magnetic moment. The 4*d* shell is almost non-magnetic. The charge on 3*d* and 4*p* shells increases by 0.77–1.97 and 0.03–2.41 *e* respectively. Especially, the charge on the 4*p* orbital increases with the increase of the clusters size. A very few charge is found on the 4*d* orbit of V atom in Ag_nV ($n = 4$–12) cluster. Nevertheless, the charge on 4*s* shell reduces by 1.02–1.54 *e*. The charge transfer hints that V atom in Ag_nV clusters has a hybridization among *s*, *p*, and *d* shells. As we know, the isolated V atom has five valence electrons. At the same time, the charge of V atom in Ag_nV cluster can be obtained from Table 5. From the principle of charge conservation, 0.10–0.21 *e* transfer from V atom to Ag atoms for the planar Ag_nV ($n = 1$–4) clusters, whereas 0.35–2.92 *e* from Ag atoms to V atom for the 3D Ag_nV ($n = 5$–12) clusters, as shown in Fig. 9. If *M* and *C* denote the magnetic moment and valence electron of V atom in Ag_nV clusters, both the variation of magnetic moment ($\Delta M = M - 3$) and charge transfer ($\Delta C = 5 - C$) have the same changing trend, as displayed in Fig. 10. It can be concluded from Fig. 10 that charge transfer should be the reason for the modification of the magnetic moment of V atom in Ag_nV clusters.

Conclusions

The structural, electronic, and magnetic properties of Ag_nV ($n = 1$–12) clusters have been investigated on the basis of DFT and CALYPSO structure searching method. The results indicate V atom in the lowest energy Ag_nV cluster tends to occupy the position with the highest coordination number. The substitution of an Ag atom in Ag_{n+1} ($n \geq 5$) cluster by one V atom changes the geometry of the host clusters. The infrared spectra, Raman spectra, and PES of Ag_nV ($n = 1$–12) clusters are expected to identify the ground states in times to come. Aside from AgV, the stability of other Ag_nV cluster is higher than that of Ag_{n+1} cluster. The relatively easy dissociation channels are $Ag_nV = Ag + Ag_{n-1}V$ for $n = 1$ and 4–12 and $Ag_nV = Ag_2 + Ag_{n-2}V$ for $n = 2$ and 3. The chemical activity of Ag_nV cluster with odd *n* is higher than that of Ag_{n+1} clusters. The magnetic moments of Ag_nV clusters originate mainly from the doped V atom and decrease gradually from 5 to 1 μ_B with the increase of cluster size. The change of magnetic moment may be attributed to the charge transfer between V and Ag atoms.

Abbreviations

3D: Three-dimensional; DE: Dissociation energy; DFT: Density functional theory; EA: Electron affinity; HOMO: Highest occupied molecular orbital; LUMO: Lowest unoccupied molecular orbital; PSO: Particle swarm optimization; VIP: Vertical ionization potential

Authors' Contributions

DD, RX, and Y-GX conceived the idea. RX, LX, and X-YS performed the calculations. DD and RX wrote the manuscript and all authors contributed to revisions. All authors read and approved the final manuscript.

Funding

This project was supported by the National Natural Science Foundation of China (11574220) and by Innovation Project in Sichuan Province.

Competing Interests

The authors declare that they have no competing interests.

Publisher's Note

Received: 19 October 2017 Accepted: 30 November 2017
Published online: 16 December 2017

References

1. Molina B, Tlahuice-Flores A (2016) Thiolated Au_{18} cluster: preferred Ag sites for doping, structures, and optical and chiroptical properties. Phys Chem Chem Phys 18:1397–1403
2. Gomez LF, O'Connell SMO, Jones CF, Kwok J, Vilesov AF (2016) Laser-induced reconstruction of Ag clusters in helium droplets. J Chem Phys 145:114304
3. Lethiec CM, Madison LR, Schatz GC (2016) Dependence of plasmon energies on the acoustic normal modes of Ag_n (n=20, 84, and 120) clusters. J Phys Chem C 120:20572–20578
4. Chen J, Zhang HY, Liu XH, Yuan CQ, Jia MY, Luo ZX, Yao JN (2016) Charge-transfer interactions between TCNQ and silver clusters Ag_{20} and Ag_{13}. Phys Chem Chem Phys 18:7190–7196
5. Urushizaki M, Kitazawa H, Takano S, Takahata R, Yamazoe S, Tsukuda T (2015) Synthesis and catalytic application of ag_{44} clusters supported on mesoporous carbon. J Phys Chem C 119:27483–27488
6. Buceta D, Busto N, Barone G, Leal JM, Dominguez F, Giovanetti LJ, Requejo FG, Garcia B, Lopez-Quintela MA (2015) Ag_2 and Ag_3 clusters: synthesis, characterization, and interaction with DNA. Angew Chem Int Ed 54:7612–7616
7. Van der Linden M, Barendregt A, van Bunningen AJ, Chin PTK, Thies-Weesie D, de Groot FMF, Meijerink A (2016) Characterisation, degradation and regeneration of luminescent Ag_{29} clusters in solution. Nano 8:19901–19909
8. Hakkinen H, Moseler M, Landman U (2002) Bonding in Cu, Ag, and Au clusters: relativistic effects, trends, and surprises. Phys Rev Lett 89:033401
9. Radcliffe P, Przystawik A, Diederich T, Doppner T, Tiggesbaumker J, Meiwes-Broer KH (2004) Excited-state relaxation of Ag_8 clusters embedded in helium droplets. Phys Rev Lett 92:173403
10. Ošťádal I, Kocan P, Sobotik P, Pudl J (2005) Direct observation of long-range assisted formation of Ag clusters on Si(111)7×7. Phys Rev Lett 95:146101
11. Gao JF, Zhao JJ (2012) Initial geometries, interaction mechanism and high stability of silicene on Ag(111) surface. Sci Rep 2:861
12. CL D, Wang BB, Sun F, Huang ML, He CJ, Liu YW, Zhang XJ, Shi DN (2015) Refractive index sensitivities of plane Ag nanosphere cluster sensors. Sensor Actuat B-Chem 215:142–145
13. Petty JT, Sergev OO, Ganguly M, Rankine IJ, Chevrier DM, Zhang P (2016) A segregated, partially oxidized, and compact Ag_{10} cluster within an encapsulating DNA host. J Am Chem Soc 138:3469–3477
14. DK H, He X, Sun LF, GC X, Jiao LY, Zhao L (2016) Growth of single-walled carbon nanotubes from Ag_{15} cluster catalysts. Sci Bull 61:917–920

15. McKee ML, Samokhvalov A (2017) Density functional study of neutral and charged silver clusters Ag_n with n=2-22 evolution of properties and structure. J Phys Chem A 121:5018–5028
16. Feng DL, Feng YH, Yuan SW, Zhang XX, Wang G (2017) Melting behavior of Ag nanoparticles and their clusters. Appl Therm Eng 111:1457–1463
17. Kahlal S, Liu CW, Saillard JY (2017) Ag_{13}-centered cuboctahedral architecture in inorganic cluster chemistry: a DFT investigation. Inorg Chem 56:1209–1215
18. Chen ZW, Wen Z, Jiang Q (2017) Rational design of ag_{38} cluster supported by graphdiyne for catalytic CO oxidation. J Phys Chem C 121:3463–3468
19. Chen PT, Tyo EC, Hayashi M, Pellin MJ, Safonova O, Nachtegaal M, van Bokhoven JA, Vajda S, Zapol P (2017) Size-selective reactivity of subnanometer Ag_4 and Ag_{16} clusters on a TiO_2 surface. J Phys Chem C 121:6614–6625
20. Liao MS, Watts JD, Huang MJ (2014) Theoretical comparative study of oxygen adsorption on neutral and anionic Ag_n and Au_n clusters (n=2-25). J Phys Chem C 118:21911–21927
21. Zhang CX, Chen CH, Dong HX, Shen JR, Dau H, Zhao JQ (2015) A synthetic Mn_4Ca-cluster mimicking the oxygen-evolving center of photosynthesis. Science 348:690–693
22. Hadipour NL, Peyghan AA, Soleymanabadi H (2015) Theoretical study on the Al-doped ZnO nanoclusters for CO chemical sensors. J Phys Chem C 119:6398–6404
23. Chi YH, Zhao LM, XQ L, An CH, Guo WY, CML W (2016) Effect of alloying on the stabilities and catalytic properties of Ag-Au bimetallic subnanoclusters: a theoretical investigation. J Mater Sci 51:5046–5060
24. Kahnouji H, Najafvandzadeh H, Hashemifar SJ, Alaei M, Akbarzadeh H (2015) Density-functional study of the pure and palladium doped small copper and silver clusters. Chem Phys Lett 630:101–105
25. Zhao YR, Zhang HR, Zhang MG, Zheng BB, Kuang XY (2014) DFT study of size-dependent geometries, stabilities and electronic properties of Si_2Ag_n clusters: comparison with pure silver clusters. Mol Phys 112:972–981
26. Li YJ, Lyon JT, Woodham AP, Fielicke A, Janssens E (2014) The geometric structure of silver-doped silicon clusters. ChemPhysChem 15:328–336
27. Wang HQ, Kuang XY, Li HF (2009) Structural, electronic, and magnetic properties of gold cluster anions doped with zinc: $AunZn^-$ (2≤ n≤10) J Phys Chem A 113:14022-14028
28. Xia XX, Kuang XY, Lu C, Jin YY, Xing XD, Merino G, Hermann A (2016) Deciphering the structural evolution and electronic properties of magnesium clusters: an aromatic homonuclear metal Mg_{17} cluster. J Phys Chem A 120:7947–7954
29. Gao Y, Liu XZ, Wang ZG (2017) $Ce@Au_{14}$: a bimetallic superatom cluster with 18-electron rule. J Electron Mater 46:3899–3903
30. Hirsch K, Zamudio-Bayer V, Langenberg A, Niemeyer M, Langbehn B, Moller T, Terasaki A, von Issendorff B, Lau JT (2015) Magnetic moments of chromium-doped gold clusters: the anderson impurity model in finite systems. Phys Rev Lett 114:087202
31. Wang HQ, Li HF (2014) A combined stochastic search and density functional theory study on the neutral and charged silicon-based clusters MSi_6 (M=La, Ce, Yb and Lu). RSC Adv 4:29782–29793
32. Ghanty TK, Banerjee A, Chakrabarti A (2010) A structures and the electronic properties of $Au_{19}X$ clusters (X=Li, Na, K, Rb, Cs, Cu, and Ag). J Phys Chem C 114:20–27
33. Joshi K, Krishnamurty S (2017) Thermo-stimuli response of doped MAu_n^- clusters (n=4-8; M=Si, Ge) at discrete temperatures: a BOMD undertaking. J Phys Chem C 121:17514–17522
34. Jaiswal S, Kumar V (2015) Growth behavior and electronic structure of neutral and anion $ZrGe_n$ (n=1–21) clusters. Comput Theor Chem 1075:87–97
35. Kwak K, Tang Q, Kim M, Jiang DE, Lee D (2015) Interconversion between superatomic 6-electron and 8-electron configurations of $M@Au_{24}(SR)_{18}$ clusters (M=Pd, Pt). J Am Chem Soc 137:10833–10840
36. Zeng WP, Tang J, Wang P, Pei Y (2016) Density functional theory (DFT) studies of CO oxidation reaction on M_{13} and $Au_{18}M$ clusters (M=Au, Ag, Cu, Pt and Pd): the role of co-adsorbed CO molecule. RSC Adv 6:55867–55877
37. Xing XD, Hermann A, Kuang XY, Ju M, Lu C, Jin YY, Xia XX, Maroulis G (2015) Insights into the geometries, electronic and magnetic properties of neutral and charged palladium clusters. Sci Rep 6:19656
38. Xia XX, Hermann A, Kuang XY, Jin YY, Lu C, Xing XD (2016) Study of the structural and electronic properties of neutral and charged niobium-doped silicon clusters: niobium encapsulated in silicon cages. J Phys Chem C 120:677–684
39. Jin YY, Tian YH, Kuang XY, Zhang CZ, Lu C, Wang JJ, Lv J, Ding LP, Ju M (2015) Ab initio search for global minimum structures of pure and boron doped silver clusters. J Phys Chem A 119:6738–6745
40. Jin YY, Maroulis G, Kuang XY, Ding LP, Lu C, Wang JJ, Lv J, Zhang CZ, Ju M (2015) Geometries, stabilities and fragmental channels of neutral and charged sulfur clusters: S_n^Q (n=3–20, Q =0, ±1). Phys Chem Chem Phys 17:13590
41. Ju M, Lv J, Kuang XY, Ding LP, Lu C, Wang JJ, Jin YY, Maroulis G (2015) Systematic theoretical investigation of geometries, stabilities and magnetic properties of iron oxide clusters $(FeO)_n^\mu$ (n=1–8, μ=0, ±1): insights and perspectives. RSC Adv 5:6560
42. Wang HQ, Kuang XY, Li HF (2010) Density functional study of structural and electronic properties of bimetallic copper-gold clusters: comparison with pure and doped gold clusters. Phys Chem Chem Phys 2:5156
43. Wang HQ, Li HF (2015) Structure identification of endohedral golden cage nanoclusters. RSC Adv 5:94685–94693
44. Li HF, Wang HQ (2014) Probing the stability of neutral and anionic transition-metal-doped golden cage nanoclusters: $M@Au_{16}^-$ (M=Sc, Ti, V). Phys Chem Chem Phys 16:244–254
45. Mokkath JH, Schwingenschlogl U (2014) Structural and optical properties of Si-doped Ag clusters. J Phys Chem C 118:4885–4889
46. Zhao GF, Sun JM, Zeng Z (2007) Absorption spectra and electronic structures of Au_mAg_n (m+n=8) clusters. Chem Phys 342:267–274
47. Li WY, Chen FY (2015) Alloying effect on performances of bimetallic Ag–Au cluster sensitized solar cells. J Alloy Compd 632:845–848
48. Chang L, HX X, Cheng DJ (2014) Role of ligand type on the geometric and electronic properties of Ag–Au bimetallic clusters. Comput Theor Chem 1045:35–40
49. Zhang N, Chen FY, XQ W (2015) Global optimization and oxygen dissociation on polyicosahedral $Ag_{32}Cu_6$ core-shell cluster for alkaline fuel cells. Sci Rep 5:11984
50. Ma WQ, Chen FY (2012) Optical and electronic properties of Cu doped Ag clusters. J Alloy Compd 541:79–83
51. Zhang YX, Yang ZX (2015) Tuning the catalytic activity of Ag-Pd alloy cluster for hydrogen dissociation by controlling the Pd ratio. Comput Theor Chem 1071:39–45
52. Sargolzaei M, Lotfizadeh N (2011) Spin and orbital magnetism of a single 3d transition-metal atom doped into icosahedral coinage-metal clusters X_{12} (X=Cu, Ag, Au). Phys Rev B 83:155404
53. Palagin D, Doye JPK (2016) DNA-stabilized Ag-Au bimetallic clusters: the effects of alloying and embedding on optical properties. Phys Chem Chem Phys 18:22311
54. Zhao S, Ren YL, WW L, Wang JJ, Yin WP (2012) Density functional study of H2S binding on small cationic AgnAum + (n+m≤5) clusters. Comput Theor Chem 997:70–76
55. Hussain R, Hussain AI, Chatha SAS, Mansha A, Ayu K (2017) Density functional theory study of geometric and electronic properties of full range of bimetallic Ag_nY_m (n+m=10) clusters. J Alloy Compd 705:232–246
56. Zhang M, XY G, Zhang WL, Zhao LN, He LM, Luo YH (2010) Probing the magnetic and structural properties of the 3d, 4d, 5d impurities encapsulated in an icosahedral Ag_{12} cage. Physica B 405:642–648
57. Chen L, Wang ZG, Li ZQ, Zhang RQ (2017) Chemical coupling sers properties of pyridine on silver-caged metal clusters $M@Ag_{12}$ ($M = V^-$, Nb^-, Ta^-, Cr, Mo, W, Mn^+, Tc^+, Re^+). J Electron Mater 46:3904–3909
58. Medel VM, Reber AC, Chauhan V, Sen P, Koster AM, Calaminici P, Khanna SN (2014) Nature of valence transition and spin moment in Ag_nV^+ clusters. J Am Chem Soc 136:8229–8236
59. Gong XY, WW J, Li TW, Feng ZJ, Wang Y (2015) Spin–orbit splitting and magnetism of icosahedral $M@Ag_{12}$ clusters (M =3d and 4d atoms). J Clust Sci 26:759–773
60. Frisch MJ, Trucks GW, Schlegel HB, Scuseria GE, Robb MA, Cheeseman JR, Montgomery JA, Jr Vreven T, Kudin KN, Burant JC et al (2009) Gaussian 09 revision a 02. Gaussian Inc, Wallingford CT
61. Perdew JP, Chevary JA, Vosko SH, Jackson KA, Pederson MR, Singh DJ, Fiolhais C (1992) Atoms, molecules, solids, and surfaces: applications of the generalized gradient approximation for exchange and correlation. Phys Rev B 46:6671–6687
62. Hay PJ, Wadt WR (1985) Ab initio effective core potentials for molecular calculations potentials for K to Au including the outermost core orbitals. J Chem Phys 82:299–311
63. Wang Y, Lv J, Zhu L, Ma Y (2010) Crystal structure prediction via particle-swarm optimization. Phys Rev B 82:094116

64. Janssens E, Neukermans S, Wang X, Veldeman N, Silverans RE, Lievens P (2005) Stability patterns of transition metal doped silver clusters: dopant- and size-dependent electron delocalization. Eur Phys J D 34:23–27
65. Janssens E, Neukermans S, Nguyen HMT, Nguyen MT, Lievens P (2005) Quenching of the magnetic moment of a transition metal dopant in silver clusters. Phys Rev Lett 94:113401
66. Reed AE, Curtiss LA, Weinhold F (1988) Intermolecular interactions from a natural bond orbital, donor-acceptor viewpoint. Chem Rev 88:899–926
67. Lee HM, Ge MF, Sahu BR, Tarakeshwar P, Kim KS (2003) Geometrical and electronic structures of gold, silver, and gold-silver binary clusters: origins of ductility of gold and gold-silver alloy formation. J Phys Chem B 107:9994–10005
68. Wu X, Ray AK (1999) A density functional study of small neutral and cationic vanadium clusters V_n and V_n^+ (n=2–9). J Chem Phys 110:2437